

THE EXTREMELY WET MARCH OF 2017 IN PERU

NIKOLAOS CHRISTIDIS, RICHARD A. BETTS, AND PETER A. STOTT

While extreme rainfall of March 2017 in Peru was favored by the anomalously warm ocean, human influence is also estimated to make such events at least 1.5 times more likely.

INTRODUCTION. Peru's rainy season falls in the first quarter of the year, often dubbed the "landslide season," with the direst downpours typically occurring in March (Lavado Casimiro et al. 2012). The rains of March 2017, however, were deadlier than usual and wreaked unprecedented havoc, leaving half of the country in a state of emergency. Widespread flooding and landslides affected 1.7 million people, while the death toll reached 177 and an estimated total damage of \$3.1 billion was reported (EM-DAT 2017). Anomalously warm sea surface temperatures (SSTs) in the region, characteristic of El Niño conditions, favor extreme rainfall (Sanabria et al. 2018). Although a marked SST anomaly was present off the Peruvian coast at the time of the event (Fig. 1a), the strong global El Niño of 2015–16 had already come to an end, as demonstrated in the time series of the Southern Oscillation index (SOI; CPC 2017) shown in Fig. 1b. The ocean at the peak of the March rains was warmer than during the preceding El Niño (Fraser 2017), creating conditions that are commonly referred to as a "local" or "coastal" El Niño, also reflected in the anomalously high value of the Niño 1 + 2 index in March (Trenberth et al. 2016). A possible atmospheric triggering mechanism of the 2017 coastal warming was proposed by Garreaud (2018). While the presence of a warm SST anomaly increases the likelihood of extreme rainfall in the region, anthropogenic climate change may also make a contribution, for example, via a long-term warming of the ocean (Rhein et al. 2013)

that could intensify the local El Niño. A similarly catastrophic event associated with the El Niño of 1998 amassed more rainfall in the region, but, as reported in the media, what made March 2017 distinct was the fact that heavier rainfall fell in shorter periods. This study employs a well-established probabilistic event attribution methodology (Stott et al. 2016) to examine the effect of man-made climate change on extreme rainfall events in Peru similar to 2017, over the entire month of March, as well as on shorter, submonthly time scales.

Data and methods. Attribution analyses use classes of extreme events that share some basic characteristics with the event under investigation (Christidis et al. 2018). Here, extreme rainfall averaged over the Peruvian region (69° – 83° E, 0° – 20° S) is defined as the exceedance of a high threshold. Three climatological thresholds are employed to examine extremes of different rarity, namely the 1-in-10-, 1-in-50-, and 1-in-100-yr events during 1960–2015. This period is modeled by 15 ensemble simulations of the historical climate with HadGEM3-A, the model underpinning the Hadley Centre's event attribution system (Christidis et al. 2013; Ciavarella et al. 2018). Different event durations are also considered by computing the average rainfall over the month of March, the 10 and 5 wettest consecutive days in March (R10x and R05x), and the wettest day of that month (R01x). The monthly mean anomaly pattern in March 2017 computed with data from the NCEP–NCAR reanalysis (Kalnay et al. 1996) is illustrated in Fig. 1c. The total rainfall over the reference region is about 5 standard deviations above the historical mean estimated with the reanalysis data and this is also the case in subregions over the mountains and to the east of the Andes (see the online supplemental material). March rainfall time series constructed with NCEP–NCAR and HadGEM3-A data are shown in Fig. 1d. Year 2017 stands out as a record in the reanalysis, which is also found to be the case in the shorter GPCP dataset (Huffman et al. 2009), but not in the GPCC record

AFFILIATIONS: CHRISTIDIS, BETTS, AND STOTT—Met Office Hadley Centre, Exeter, United Kingdom

CORRESPONDING AUTHOR: Nikolaos Christidis, nikos.christidis@metoffice.gov.uk

DOI:10.1175/BAMS-D-18-0110.1

A supplement to this article is available online (10.1175/BAMS-D-18-0110.2)

© 2018 American Meteorological Society

For information regarding reuse of this content and general copyright information, consult the [AMS Copyright Policy](#).

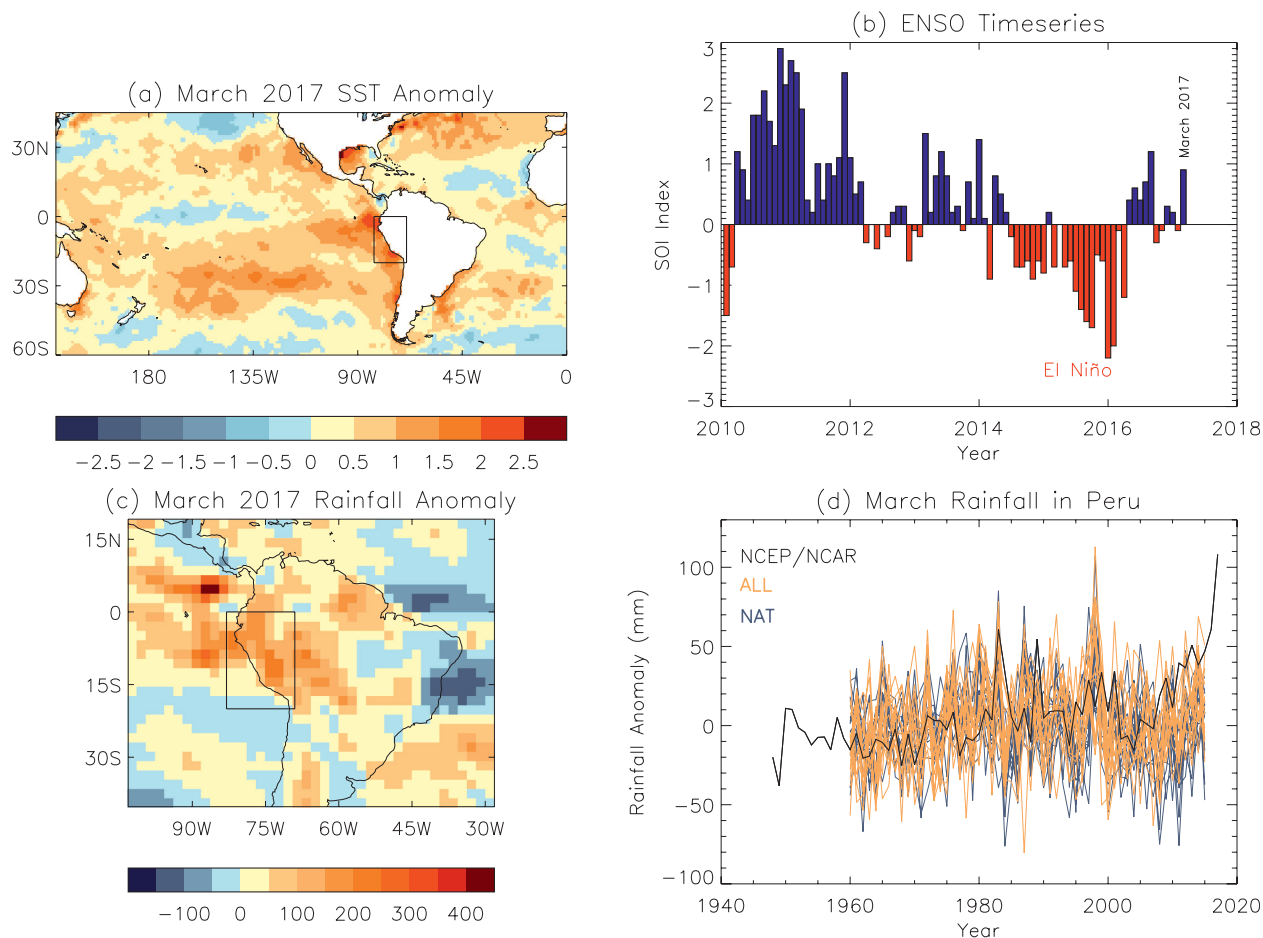


FIG. 1. (a) Mean SST anomalies ($^{\circ}\text{C}$) in March 2017 from HadISST. (b) Time series of monthly SOI values in recent years. Negative values (in red) indicate El Niño and positive values (in blue) La Niña conditions. (c) Mean rainfall anomalies (mm) in March 2017 estimated with NCEP–NCAR reanalysis data. (d) Time series of the March mean rainfall anomaly in the region of Peru constructed with NCEP–NCAR reanalysis data (black line) and HadGEM3-A data from the ALL (orange lines) and NAT (blue lines) multidecadal simulations. All anomalies are relative to 1961–90. The black box in (a) and (b) marks the study area.

(Schneider et al. 2016). Rainfall over shorter time scales (R10x, R05x, R01x) is found to reach record levels in 2017 as well. Time series from the long (multidecadal) HadGEM3-A simulations are also shown in Fig. 1d. In addition to the experiment representing the historical climate that includes all (both natural and anthropogenic) external forcings (experiment ALL), a second set of 15 simulations has also been produced, representing a hypothetical natural climate without anthropogenic forcings (NAT). HadGEM3-A is an atmospheric model and therefore oceanic conditions need to be prescribed. In the ALL experiment these come from the HadISST dataset (Rayner et al. 2003). In the NAT simulations, an estimate of the anthropogenic SST change is subtracted from the observations, obtained from simulations with 19 coupled models (<http://portal.nerc.gov/c20c/experiment.html>) and simple empirical relationships are used to adjust the sea

ice to cooler SSTs (Christidis et al. 2013). The rainfall time series display characteristic peaks during major El Niño events (e.g., 1982/83), also evident in the model simulations which retain the ENSO signal through the prescribed boundary conditions. Interestingly, the 1997/98 El Niño, which had devastating impacts in Peru, is more pronounced in the model, probably indicating a reanalysis shortcoming.

This study addresses two questions: 1) Has anthropogenic influence altered the likelihood of the 2017 extreme rainfall in Peru, given the warm oceanic anomaly present at the time? 2) How does the presence of such an SST anomaly affect the current likelihood of extreme rainfall in the region? To answer these questions the Hadley Centre’s event attribution system is employed. Large 525-member ensembles of ALL and NAT simulations of the first quarter of 2017 were generated, as part of the sys-

tem's quasi-operational setup. The coastal El Niño is also manifest in the NAT simulations, although the cooler ocean under preindustrial conditions takes the edge off the intensity of the 2017 anomaly (see the online supplemental material). The first question of the study is addressed by comparing estimated probabilities of extremes obtained with the ALL and NAT simulations of March 2017 (525 estimates per experiment). The impact of the coastal El Niño in the present-day climate is examined by comparing the 525 ALL simulations for 2017 with their counterparts of the historical climate, from which the last 10 years (2006–15) are extracted. The selected years provide a sample of 150 (15 runs × 10 yr) probability estimates and are used as a proxy of the current climate under any oceanic conditions. Near-zero mean March SST anomalies over this decade (see the supplemental material) indicate no SST bias in the near-present-day climate. As in previous work, extreme probabilities are computed with the generalized Pareto distribution and their associated uncertainties with a Monte Carlo bootstrap procedure (Christidis et al. 2013). It is essential that models in attribution studies are evaluated to establish whether they are fit for the purpose (Vautard et al. 2018). Despite the lack of long and reliable observational rainfall records for Peru available to the authors, standard evaluation assessments against reanalysis data applied to HadGEM3-A indicate that the model's representation of rainfall variability and extremes in the region is consistent with the reanalysis (see the supplemental material).

While it cannot be established beyond doubt that the modeled rainfall over the complex topography of the study region is reliable, the attribution results presented below ought to be viewed in the light of this uncertainty.

Results. Return times (reverse probabilities) of extreme rainfall events are reported in Table 1. A comparison between the ALL and NAT estimates for 2017 indicates that anthropogenic forcings unambiguously increase the likelihood of extremes across events of different rarity and duration. Human influence leads to a shift in the March rainfall distribution illustrated in Fig. 2a (similar shifts also found for shorter rainfall durations). The estimated risk ratios plotted in Fig. 2b reveal greater anthropogenic influence on rarer events (1 in 100 yr), although the uncertainty in the likelihood of these events also increases. The effect of the warm SSTs is inferred by comparing ALL simulations of 2017, when a strong anomaly was present, with ALL simulations of recent years representing a wider range of oceanic conditions. Figures 2c and 2d show that the SST anomaly of 2017 leads to a marked shift in the rainfall distribution and in most cases increases the likelihood of extremes by at least a factor of 3. The probabilities of the rarer events without the effect of a strong SST anomaly are very small and hence their estimates suffer from large uncertainties (Table 1). Risk ratios estimated in subregions with different topography indicate no peculiar orographic effect on the attribution findings (supplemental material). It should be noted that

TABLE 1. Return times (in years) of high rainfall events in Peru estimated using the ALL and NAT experiments for year 2017 and the multidecadal ALL simulations for years 2006–15. Estimates are provided for the total rainfall in March, the 10 and 5 wettest consecutive days, and the wettest day in March. The best estimate (50th percentile) of the return time is reported together with the 5%–95% uncertainty range (in parentheses).

	March	R10x	R05x	R01x
1-in-10-yr events				
ALL 2017	1.99 (1.85 to 2.14)	2.10 (1.95 to 2.27)	2.22 (2.06 to 2.43)	3.62 (3.14 to 4.08)
NAT 2017	3.44 (3.08 to 3.90)	3.40 (3.05 to 3.83)	4.26 (3.79 to 4.74)	6.91 (5.88 to 8.25)
ALL 2006–15	10.23 (6.88 to 17.08)	9.41 (7.02 to 13.65)	12.25 (7.48 to 19.40)	10.39 (5.75 to 22.64)
1-in-50-yr events				
ALL 2017	6.02 (5.23 to 6.98)	8.71 (7.45 to 10.22)	10.19 (8.71 to 12.24)	14.48 (11.78 to 18.47)
NAT 2017	19.51 (15.33 to 25.97)	22.02 (17.10 to 29.91)	46.92 (33.06 to 72.72)	34.92 (25.43 to 51.07)
ALL 2006–15	Large uncertainty (45 to >10 ⁴)			
1-in-100-yr events				
ALL 2017	12.09 (9.60 to 15.46)	19.25 (15.46 to 25.27)	23.97 (18.88 to 32.46)	20.23 (15.89 to 26.56)
NAT 2017	55.28 (40.02 to 88.93)	74.26 (49.45 to 131)	1945 (523 to >10 ⁴)	56.93 (39.13 to 96.06)
ALL 2006–15	Large uncertainty (100 to >10 ⁴)			

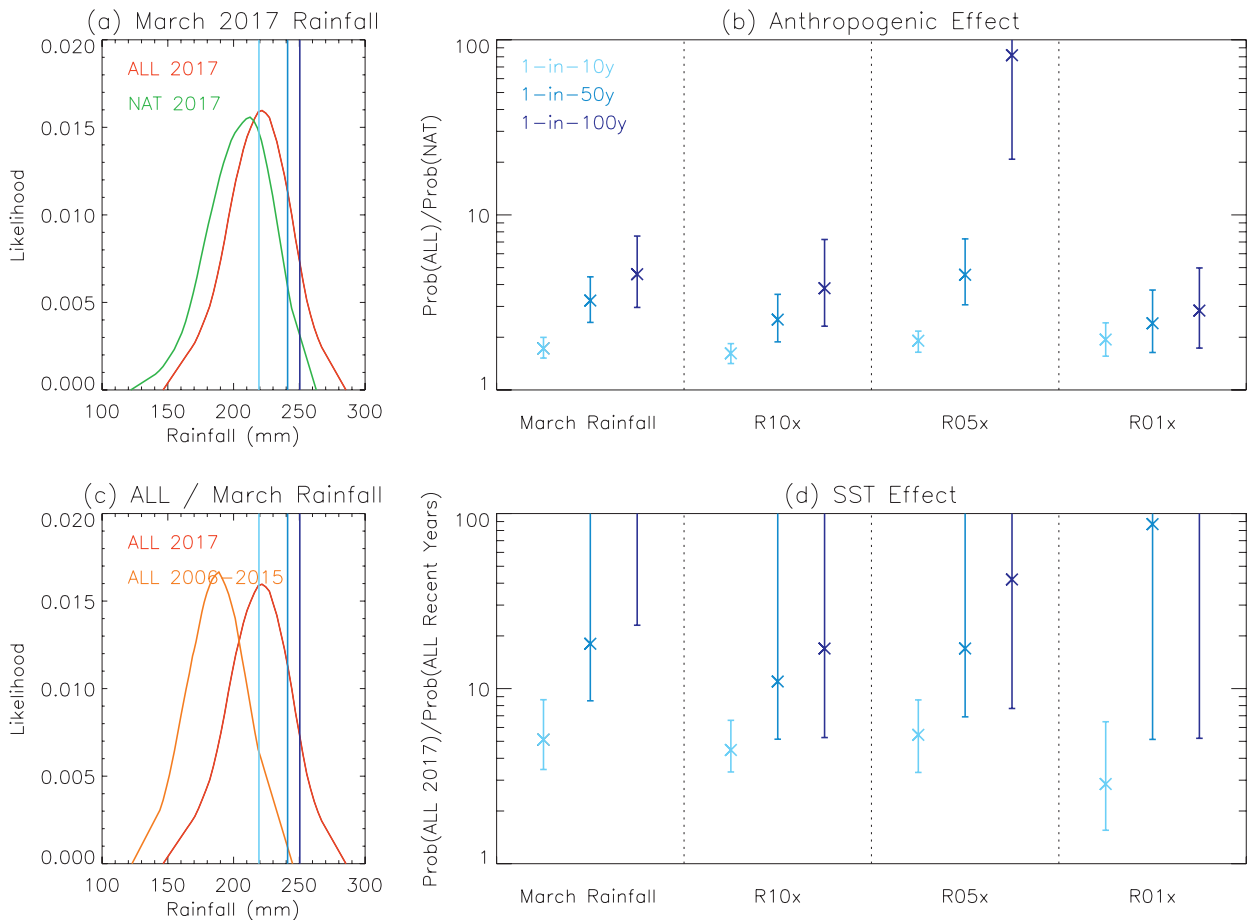


FIG. 2. (a) Normalized distributions of the March 2017 mean rainfall in Peru constructed with data from the ALL (red) and NAT (green) experiments. Events with different climatological return times (1-in-10-, 1-in-50-, and 1-in-100-yr) are represented by the vertical blue lines. (b) Risk ratio estimates showing the effect of human influence on March rainfall, R10x, R05, and R01x extremes. Events with different climatological return times are represented by different shades of blue. The best estimate (50th percentile) is marked by a cross and the 5%–95% uncertainty range by whiskers. (c) As in (a), but for distributions constructed with data from the ALL experiments for March 2017 (red line) and the same month in years 2006–15 (orange line). (d) As in (b), but for the effect of the 2017 SST anomalies on rainfall extremes.

uncertainties related to the boundary conditions and model’s ability to represent regional rainfall are also present and will affect to some extent the attribution results shown here.

Conclusions. Coastal El Niño conditions and man-made climate change both favor extreme rainfall in Peru. When the effect of large positive SST anomalies similar to 2017 is factored in, wet extremes are estimated to be at least 1.5 times more likely to happen (or 2–3 times for more rare events) compared to pre-industrial times. The coastal El Niño is estimated to increase the likelihood of extremes 3–6 times (best estimate), or more than 10 times for rarer events. Although model dependency, and in particular the uncertainty in the NAT boundary conditions, may affect the estimated probabilities (Christidis and

Stott 2014), it was verified that the modeled oceanic warming used in this study to produce the boundary conditions is broadly consistent with observed SST trends in the region, which increases confidence in the results. Uncertainty about the accuracy of the simulated rainfall in the region remains the major caveat of this study, traced to the lack of reliable observational datasets for a detailed model evaluation. Hence, the attribution results reported here only provide a useful first assessment of the event’s main drivers rather than a definitive measure of their effect. Moving toward the integration of the Hadley system into an attribution service that outputs assessments of extremes on a regular basis, could be key to well-informed decision-making, especially in the aftermath of catastrophic events like the one investigated here.

ACKNOWLEDGMENTS. This work was supported by the Joint DECC/Defra Met Office Hadley Centre Climate Programme (GA01101) and the EUPHEME project, which is part of ERA4CS, an ERA-NET initiated by JPI Climate and co-funded by the European Union (Grant 690462).

REFERENCES

- Christidis, N., and P. A. Stott, 2014: Change in the odds of warm years and seasons due to anthropogenic influence on the climate. *J. Climate*, **27**, 2607–2621, <https://doi.org/10.1175/JCLI-D-13-00563.1>.
- , —, A. Scaife, A. Arribas, G. S. Jones, D. Copsey, J. R. Knight, and W. J. Tennant, 2013: A new HadGEM3-A based system for attribution of weather- and climate-related extreme events. *J. Climate*, **26**, 2756–2783, <https://doi.org/10.1175/JCLI-D-12-00169.1>.
- , A. Ciavarella, and P. A. Stott, 2018: Different ways of framing event attribution questions: The example of warm and wet winters in the United Kingdom similar to 2015/16. *J. Climate*, **31**, 4827–4845, <https://doi.org/10.1175/JCLI-D-17-0464.1>.
- Ciavarella, A., and Coauthors, 2018: Upgrade of the HadGEM3-A based attribution system to high resolution and a new validation framework for probabilistic event attribution. *Wea. Climate Extremes*, **20**, 9–32, <https://doi.org/10.1016/j.wace.2018.03.003>.
- CPC, 2017: Southern Oscillation Index (SOI): (Stand Tahiti—Stand Darwin) sea level pressure data. Climate Prediction Center, accessed June 2017, www.cpc.ncep.noaa.gov/data/indices/soi.
- EM-DAT, 2017: The Emergency Events Database. Centre for Research on the Epidemiology of Disasters, accessed December 2017, www.emdat.be.
- Fraser, B., 2017: Peru's floods teach tough lessons. *Nature*, **544**, 405–406, <https://doi.org/10.1038/544405a>.
- Garreaud, R., 2018: A plausible atmospheric trigger for the 2017 coastal El Niño. *Int. J. Climatol.*, **38**, e1296–e1302, <https://doi.org/10.1002/joc.5426>.
- Huffman, G. J., R. F. Adler, D. T. Bolvin, and G. Gu, 2009: Improving the global precipitation record: GPCP version 2.1. *Geophys. Res. Lett.*, **36**, L17808, <https://doi.org/10.1029/2009GL040000>.
- Kalnay, E., and Coauthors, 1996: The NCEP/NCAR 40-Year Reanalysis Project. *Bull. Amer. Meteor. Soc.*, **77**, 437–471, [https://doi.org/10.1175/1520-0477\(1996\)077<0437:TNYRP>2.0.CO;2](https://doi.org/10.1175/1520-0477(1996)077<0437:TNYRP>2.0.CO;2).
- Lavado Casimiro, W. S., J. Ronchail, D. L. Labat, J. C. Espinoza, and J. L. Guyot, 2012: Basin-scale analysis of rainfall and runoff in Peru (1969–2004): Pacific, Titicaca and Amazonas drainages. *Hydrol. Sci. J.*, **57**, 625–642, <https://doi.org/10.1080/02626667.2012.672985>.
- Rayner, N. A., D. E. Parker, E. B. Horton, C. K. Folland, L. V. Alexander, D. P. Rowell, E. C. Kent, and A. Kaplan, 2003: Global analyses of sea surface temperature, sea ice, and night marine air temperature since the late nineteenth century. *J. Geophys. Res.*, **108**, 4407, <https://doi.org/10.1029/2002JD002670>.
- Rhein, M., and Coauthors, 2013: Observations: Ocean. *Climate Change 2013: The Physical Science Basis*, T. F. Stocker et al., Eds., Cambridge University Press, 255–315.
- Sanabria, J., L. Bourrel, B. Dewitte, F. Frappart, P. Rau, O. Solis, and D. Labat, 2018: Rainfall along the coast of Peru during strong El Niño events. *Int. J. Climatol.*, **38**, 1737–1747, <https://doi.org/10.1002/joc.5292>.
- Schneider, U., M. Ziese, A. Meyer-Christoffer, P. Finger, E. Rustemeier, and A. Becker, 2016: The new portfolio of global precipitation data products of the Global Precipitation Climatology Centre suitable to assess and quantify the global water cycle and resources. *Proc. IAHS*, **374**, 29–34, <https://doi.org/10.5194/piahs-374-29-2016>.
- Stott, P. A., and Coauthors, 2016: Attribution of extreme weather and climate-related events. *Wiley Interdiscip. Rev.: Climate Change*, **7**, 23–41, <https://doi.org/10.1002/wcc.380>.
- Trenberth, K., and Coauthors, Eds., 2016: The Climate Data Guide: Niño SST Indices (Niño 1+2, 3, 3.4, 4; ONI and TNI). NCAR/UCAR, accessed March 2018, <https://climatedataguide.ucar.edu/climate-data/nino-sst-indices-nino-12-3-34-4-oni-and-tni>.
- Vautard, R., and Coauthors, 2018: Evaluation of the HadGEM3-A simulations in view of detection and attribution of human influence on extreme events in Europe. *Climate Dyn.*, <https://doi.org/10.1007/s00382-018-4183-6>.